Stability and Electron Affinities of Negatively Charged Aluminium Clusters: A Computational Study

Alexander Goldberg

Accelrys, Inc., 10188 Telesis Court, San Diego, CA 92121, USA

Josep M. Oliva*

Instituto de Química-Física "Rocasolano", CSIC, Serrano, 119, E-28006 Madrid, Spain

Noelle Walsh, Franklin Martinez, Gerrit Marx, and Lutz Schweikhard

Institut für Physik, Ernst-Moritz-Arndt-Universität Greifswald, D-17487 Greifswald, Germany

Antonio Fernández-Barbero

Group of Complex Fluid Physics, University of Almeria, 04120-Almeria, Spain

Estabilidad y afinidades electrónicas de agregados de aluminio con carga negativa: un estudio computacional

Estabilitat i afinitats electròniques d'agregats d'alumini amb càrrega negativa: un estudi computacional

RESUMEN

Se presenta un estudio computacional sobre la estabilidad de agregados de aluminio, Al_n^z, neutros y cargados, con n = {13, 18, 23, 39, 55}, y z = {0, -1, -2}. Las estimaciones de afinidades electrónicas (AE) se realizaron con (i) cálculos mecánico-cuánticos con todos los electrones y optimización completa de geometría sobre los agregados Al_n^z, con n = {13, 18, 23, 39, 55}, z = {0, -1, -2}, y el funcional DFT de Perdew-Burke-Ernzerhof (PBE), el cual incluye correcciones de gradiente de la densidad, y (ii) el modelo de esfera conductora cargada con y sin barreras de Coulomb y correcciones de efecto túnel. Si consideramos como único criterio para la producción y observación experimental de agregados dianiónicos de aluminio un valor positivo de la segunda afinidad electrónica, entonces el tamaño mínimo (es decir, de número de átomos) del agregado se predice con $n \sim 23$ y $n \sim 32$ mediante las computaciones con todos los electrones y con el modelo de esfera cargada conductora respectivamente.

Palabras clave: Agregados; Aluminio; Trampa de Agregados; Trampa de Penning; DFT; Modelo de Esfera Conductora Cargada; Barrera de Coulomb; Efecto Tunel

ABSTRACT

A computational study on the stability of neutral, singly and doubly negatively charged aluminium clusters Al_n^z, with n = {13, 18, 23, 39, 55}, and z = {0, -1, -2} is presented. Estimates of electron affinities (EA) were computed with (i) all-electron quantum-mechanical calculations with full geometry optimization on Al_n^z, with n = {13, 18, 23, 39, 55}, and z = {0, -1, -2}, using the Perdew-Burke-Ernzerhof (PBE) gradient-corrected functional within Density Functional Theory (DFT) and (ii) Charged Conducting-Sphere Model with and without Coulomb barrier and tunnelling corrections. If a positive value for the second electron affinity of the cluster is considered to be the sole criterion for the production and experimental observation of dianionic aluminium clusters, then the predicted minimum cluster size (i.e. the number of atoms) is $n \sim 23$ and $n \sim 32$ from the all-electron computations and the charged conducting-sphere model, respectively.

Key words:Clusters; Aluminium; ClusterTrap; Penning Trap; DFT; Charged Conducting-Sphere Model; Coulomb Barrier; Tunneling

RESUM

Es presenta un estudi computacional sobre l'estabilitat d'agregats d'alumini, Al_n^z, neutres i amb càrrega, amb n = {13, 18, 23, 39, 55}, i z = {0, -1, -2}. Les estimacions d'afinitats electròniques (AE) es realitzen amb (i) càlculs mecànic-cuàntics amb tots els electrons i optimització completa de geometria en els agregats Al_n^z, amb n = {13, 18, 23, 39, 55}, z = {0, -1, -2}, i el funcional DFT de Perdew-Burke-Ernzerhof (PBE), el qual inclou correccions de gradient de la densitat, i (ii) el model d'esfera conductora carregada amb i sense barreres de Coulomb i correccions d'efecte túnel. Si considerem com a únic criteri per a la producció i observació experimental d'agregats dianiònics d'alumini un valor positiu de la segona afinitat electrònica, aleshores el tamany mínim (es a dir, de nombre d'àtoms) de l'agregat es prediu amb $n \sim 23$ i $n \sim 32$ mitjançant les computacions amb tots els electrons i amb el model d'esfera carregada conductora respectivament.

Mots clau: Agregats; Alumini; Trampa d'Agregats; Trampa de Penning; DFT; Model d'Esfera Conductora Carregada; Barrera de Coulomb; Efecte Tunel

*Corresponding authors:

Josep M. Oliva: J.M.Oliva@iqfr.csic.es

1. INTRODUCTION

Atomic clusters range in size from very small dimers to much larger aggregates containing up to 10^6 atoms. Due to their 'scalability', they offer the opportunity to investigate the evolution of chemical and physical properties as a function of size. Properties of particular interest include the atomic bonding parameters and the stability of polyanionic species [1]. Metal clusters are highly reactive systems and ion traps facilitate their investigation as pure species in the gas phase [2]. In the particular case of aluminium clusters [3] and their anions [4], comprehensive experimental and theoretical works on their stability [5,6], structure [7] and spectroscopic properties [8,9] have been performed within the last three decades. Clusters in the gas phase are important in chemistry due to the extended fields of research and application, such as size selection of supported metal clusters for electrocatalysis, chemical reactivity, catalytic effects, and molecular chemisorption (e.g. CO, H_2, O_2) [10]. Additional reports on the formation and stability of clusters MAl_4^- (M = Li, Na, Cu) [11] and $Al_{13}I_x^-$, $Al_{14}I_x^-$ [12,13] also indicate the potential synthetic utility of superatom chemistry using aluminium clusters. The recent detection of dianions, trianions and tetra-anions of aluminium clusters in a Penning trap [14] provides insight into the rich chemical-physics of these elusive species. Questions like "What is the minimum size n for which Al_n^{2-} can be observed?" or "What are the finite-size effects in Al_n^{2-} as compared to Al_n^{1-}?" have led to this computational work. The presentation is organised as follows: Section 2 describes the theoretical approach and section 3 contains the results and discussion, where we focus on the electronic structure of the selected clusters and compare the charged conducting-sphere model with the all-electron quantum-mechanical predictions and highlight the main differences.

2 COMPUTATIONAL MODEL

2.1 Quantum-Mechanical Density-Functional Theory (DFT) Computations:
All-electron computations were performed with the DFT code DMol³, a code that uses numerical basis sets [15]. We used version 4.0 of the program which is a part of the Materials Studio Modeling suite provided by Accelrys [16]. In the present study, the basis set used consists of a double numerical (DND) set including all occupied atomic orbitals, a second set of valence atomic orbitals and polarized d-valence orbitals. The Perdew-Burke-Ernzerhof (PBE) gradient corrected functional, which depends on the electron density and its derivative was used [17]. This functional, based on the Perdew model to correct for the local-density approximation [18], provides a correction which leaves only 1% error in exchange energy; it has a strong physical background, reliable numerical performance and is frequently used in DFT calculations. The spin unrestricted approach was applied with all electrons being considered explicitly. In all calculations, atom-centred grids were used for the numerical integration with the "Fine" option in DMol³ which includes about 2000 grid points for each atom. The real space cut-off of 7.0 Å was imposed for numerical integration [19]. The Self-Consistent-Field (SCF) convergence criterion was set to the root-mean-square change in the electronic density to be less than 10^{-6} electron/Å³. Geometries were optimized using an efficient algorithm which takes advantage of delocalized internal coordinates [20]. The convergence thresholds applied for geometry optimization were 10^{-5} atomic units (au, Hartree) for energy, 0.002 au/Å for force and 0.005 Å for displacement [21]. A frequency analysis on all optimized geometries showed positive values and therefore all geometries reported in this work correspond to energy minima [22]. In all computations the point group symmetry was imposed on the structures of aluminium clusters.

2.2 The Charged Conducting-Sphere Model:
The interaction between a singly-charged cluster anion and a nearby electron can be described by use of classical electrostatics. In this approach, the cluster monoanion is approximated by an isolated, charged, conducting sphere of radius $R_{cluster}$ and the electron is a point charge located at a distance r from the centre of the sphere. The Coulomb potential between the two charged particles is found by the method of image charges [23] to be

$$V_C\left(r, R_{cluster}, z\right) = \frac{e^2}{4\pi\varepsilon_0}\left(\frac{z}{r} - \frac{R_{cluster}^3}{2r^2\left(r^2 - R_{cluster}^2\right)}\right) \quad (1)$$

where z denotes the charge-state of the sphere, i.e. $z \cdot e = -|z| \cdot e$ is the charge of the precursor anion before attachment of an additional electron or
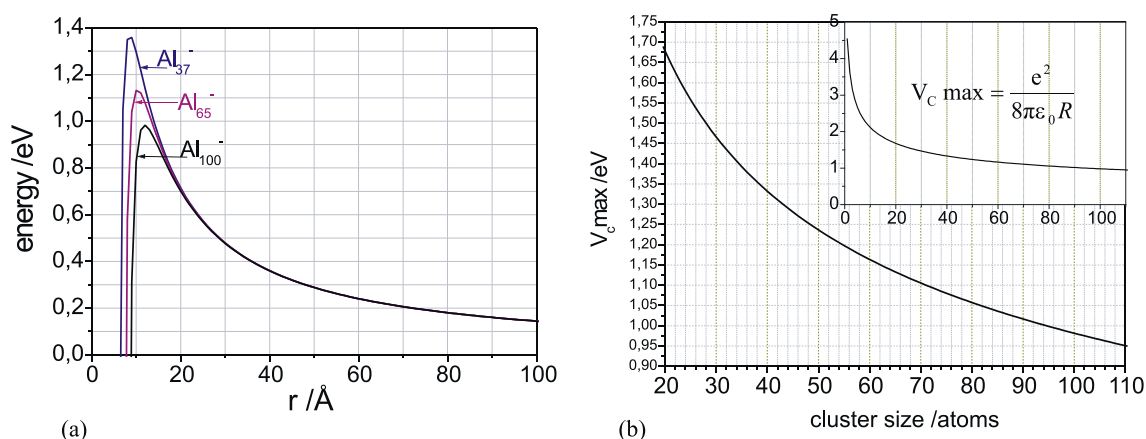

Figure 1. *(a) Coulomb barriers of cluster monoanions containing 37, 65, and 100 atoms respectively and (b) barrier height ($V_c$max) as a function of cluster size.*

$(z - 1) \cdot e = - (|z|+1) \cdot e$ is the charge of the precursor anion before emission of an electron. (To avoid sign confusion in connection with the negative charge states of the anionic species considered in this contribution, the charge state will be indicated by use of the absolute value, $|z|$, where appropriate. Note that the equations presented in this notation are only correct for anions and do not apply to cations!) The Coulomb barriers of singly charged aluminium clusters containing 37, 65 and 100 atoms, respectively, are plotted in figure 1(a) for cluster radii $R_{cluster} = R_{eff} \cdot n^{1/3}$ with the Wigner-Seitz radius of aluminium, $R_{WS} = 1.58 \times 10^{-10}$ m [24, 25, 26] as the effective atomic radius and a charge state $z = -1$ of the sphere. The maximum height of the Coulomb barrier ranges from 0.98 eV for Al_{100}^{-} to 1.36 eV for Al_{37}^{-}. Figure 1(b) shows the barrier heights as a function of cluster size. For very small clusters, $n \leq 10$, the barrier height exceeds 2eV.

In the charged conducting-sphere model, the electron affinity, EA, of a cluster containing n atoms and with charge state z (in the present case $z = -1$), can be estimated as

$$EA(n, z) = W + \left(- |z| - \alpha\right) \frac{e^2}{4\pi\varepsilon_0 R_{cluster}(n)} \quad (2)$$

where W is the bulk work function of the metal, α is a dimensionless factor and $R_{cluster} = R_{eff} n^{1/3}$ is the cluster radius as described above. Note that there has been considerable controversy in the literature about the correct value of α. Following classical electrostatic calculations, it has been proposed that $\alpha = \frac{1}{2}$ [27, 28] from the spherical condensator approach or $\alpha = \frac{5}{8}$ [29, 30] from the image potential approach. It is now generally accepted that the value of $\alpha = \frac{1}{2}$ is in fact correct and that the value of $\alpha = \frac{5}{8}$ was obtained due to an error in the theoretical image potential consideration [31, 32]. However, experimentally various values of α have been found and have been explained by quantum effects [30]. A positive value of $EA(n, z)$, indicates that a cluster of charge state z, is large enough to accept another electron, resulting in a stable (with respect to electron emission) n-atom cluster of charge state $(z - 1) \cdot e = - (|z|+1) \cdot e$. Figure 2a shows the electron affinities of monoanionic aluminium clusters containing between 25 and 65 atoms as predicted by the charged conducting-sphere model with $R_{eff} = R_{WS}$ as given above

and $W = 4.28$ eV as recently determined from experimental ionisation potentials of aluminium clusters [24]. Figure 2b depicts the expected lifetimes of aluminium cluster dianions as a function of cluster size (from 25 to 42 atoms) as predicted by the charged conducting-sphere model. For a more comprehensive explanation of the concept of metastability in aluminium polyanion clusters, the Reader is referred to section VI.A and Equations (5) and (6) from reference [14c]. For completeness, an earlier approximation [14] with $R_a = 1.431 \times 10^{-10}$ m [33] as the atomic radius of the aluminium atom are also included (crosses). As mentioned above, the larger the radius of the cluster, the more positive is its electron affinity. Indeed, using the Wigner-Seitz radius rather than the atomic radius has a large effect on the predicted dianion appearance size. Whereas for $R_{eff} = R_a$ only clusters containing $n \geq 45$ atoms (crosses) were estimated to have positive electron affinities, the use of R_{WS} as the effective atomic radius (Figure 2a) shifts that lower limit to $n \geq 33$ atoms (circles). The expected experimental dianion appearance size shifts to even smaller cluster sizes if the stabilising effect of the Coulomb barrier (Equation 1) is taken into account; whilst this inhibits the attachment of an electron to an already negatively charged species, once the electron is attached, the barrier helps to stabilise the dianion against immediate electron loss. Thus, some clusters that have slightly negative second electron affinities, for example Al_{29} to Al_{32} (see figure 2a, open circles), can form metastable dianions. In these cases, the electron, once attached to the monoanion, has insufficient energy to overcome the Coulomb barrier and it can only detach from the monoanion via tunnelling. If the cluster dianion has a lifetime greater than the typical period of an experimental cycle of 1s, it is possible to observe it at the ClusterTrap setup.

Therefore, in light of the current approximations, taking into account both the electron affinity of the monoanion and the effect of the Coulomb barrier, it is estimated that aluminium cluster dianions containing $n \geq 29$ atoms could be observed at ClusterTrap.

Note again, that the present model provides only rough approximations. The calculation of the second electron affinities is purely classical and assumes the cluster to be a metallic conducting sphere. In the case of the lifetime calculations, tunnelling of the excess electron through the Coulomb barrier of the monoanion is considered, but a
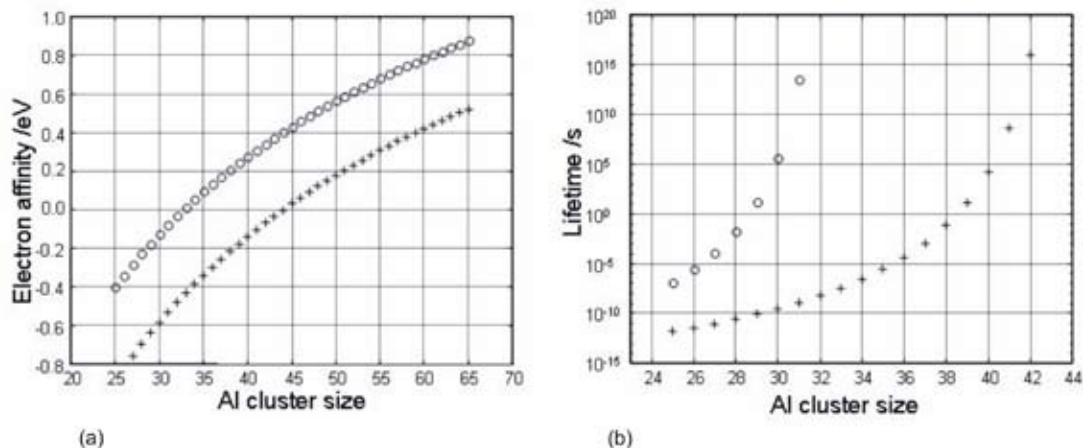

(a)

(b)

Figure 2. *(a) Electron affinity, EA, of aluminium cluster monoanions and (b) lifetimes of aluminium cluster dianions as a function of cluster size, where the effective atomic radius, R_{eff} was taken to be R_{ws} (open circles) or R_a (crosses) of the aluminium atom (see text).*

number of important phenomena have not been corrected for. Such phenomena include the deviation of the shape of the cluster from the spherical approximation, the neglect of electronic shell structure, the interaction of the electrons with one another and the "electronic spill-out" effect [34]. The discussion in Section 3 highlights the differences between the quantum mechanical DFT calculations and the charged conducting-sphere classical model.

3. RESULTS AND DISCUSSION

3.1 Electronic Structure: Table 1 gathers the computed properties of the clusters included in this work: Al_n^{-z} with ($z = 0, 1, 2$; $n = 13, 18, 23, 39, 55$).

Cluster	ε_n (eV)	IP1 (eV)	IP2(eV)	H-L gap (eV)	EA1 (eV)	EA2 (eV)
Al_{13}	2.44	6.70	10.18	1.99	2.18	-1.03
Al_{18}	2.45	5.90	8.99	0.36	2.85	-0.13
Al_{23}	2.84	5.87	8.69	0.77	3.01	0.18
Al_{39}	2.92	5.38	7.80	0.18	2.98	0.61
Al_{55}	2.99	5.33	7.54	0.45	3.13	0.94

Table 1. *Computed energetic properties of Al_n^{-z} clusters (z = 0, 1, 2; n = 13, 18, 23, 39, 55): Cluster binding energies ε_n , first and second ionization potentials (IP1 and IP2 respectively), HOMO-LUMO gaps (H-L gap) and first and second electron affinities (EA1 and EA2 respectively). DFT computations with the PBE functional and a DND basis set.*
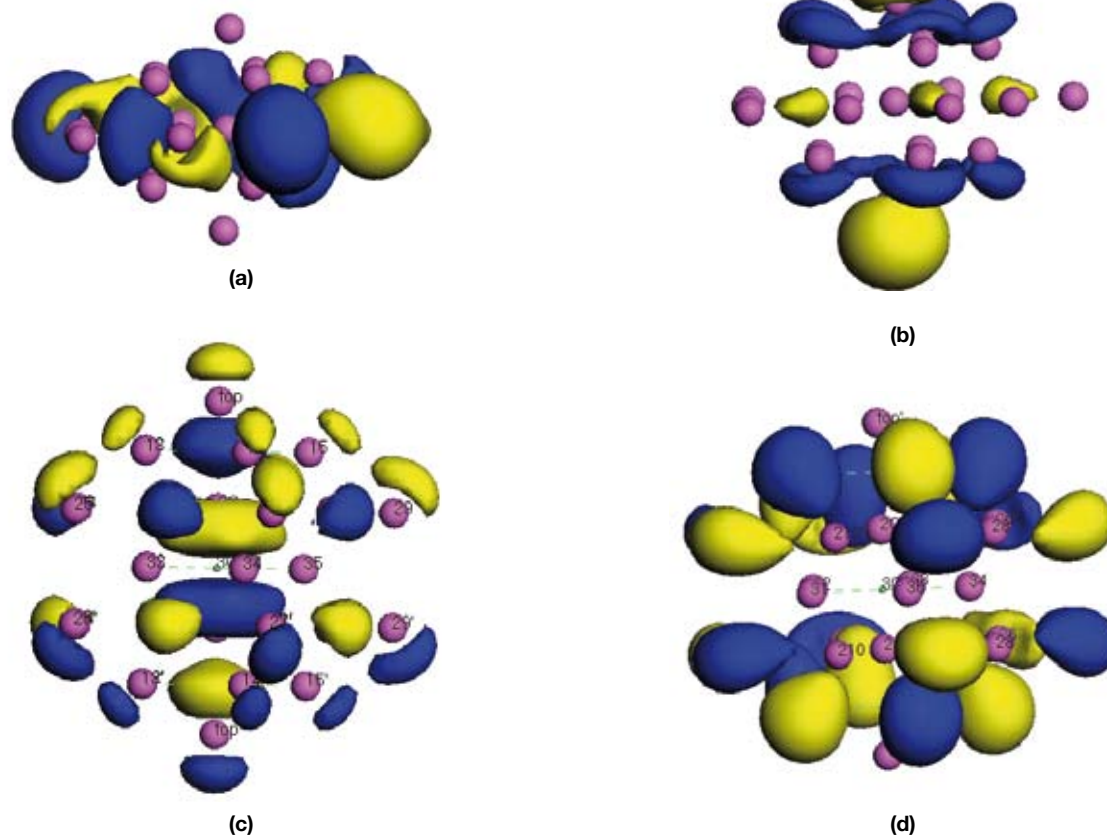
Based on the analysis of energetic properties – Table 1 – the cluster binding energies increase with cluster size, i.e.

$$\varepsilon_{13} < \varepsilon_{18} < \varepsilon_{23} < \varepsilon_{39} < \varepsilon_{55} \quad (3)$$

The average binding energy per atom – cluster binding energy – is defined as

$$\varepsilon_n = E(Al) - E(Al_n)/n. \quad (4)$$

and, according to previous computations [5], when $n \rightarrow \infty$, ε_n converges to the cohesive energy $\varepsilon_\infty = \varepsilon_{coh} = 3.35$ eV, i.e., the bulk binding energy per atom. The first and second Ionization Potentials (IP) of the clusters follow a reverse order. The cluster reactivity can be evaluated based on the HOMO-LUMO gap (Table 1). Al_{39} has the smallest HOMO-LUMO gap and therefore is predicted to be the most reactive. As regards to electron affinities (EAs), the first EAs are all positive and appear to increase with size and hence attachment of an electron can be expected. Furthermore, Al_{23} and Al_{39} are predicted to have almost the same values of *EA*1 and this could perhaps be a reflection of the enhanced stability of the Al_{23}^- cluster due to valence electron shell closure as has been predicted in Jellium computations [3]. The computed values of *EA*2 from Table 1 are further discussed below. Figure 3 shows the HOMO and LUMO orbitals for aluminium cluster anions Al_{23}^{-1} and Al_{39}^{-1}:

We have chosen these two clusters as representative of the regions where electrons can be attached to monoanioninc aluminium clusters: As will be shown below (see Sections

(a)

(b)

(c)

(d)

Figure 3. *Frontier orbitals for Al_{23}^{-1} and Al_{39}^{-1}: (a) HOMO in Al_{23}^{-1}, (b) LUMO in Al_{23}^{-1}, (c) HOMO in Al_{39}^{-1}, (d) LUMO in Al_{39}^{-1}.*

3.2 and 3.2.1), the transition point from negative to positive EA2's in Al_n^- clusters is for $n \sim 23$. As depicted in Figure 1, the HOMO and LUMO in the anion Al_{23}^{-1} is localized mainly in the equatorial and axial region of the cluster, the latter having even a more localized character on the Al atoms of the top and bottom of Al_{23}^{-1}. Therefore the excess electron in Al_{23}^{-1} is mainly localized on the equatorial region of the cluster; on the other hand, the additional electron on Al_{23}^{-2} will be attached more likely on the axial region of Al_{23}^{-1}.

Turning now to the larger cluster Al_{39}^{-1} the HOMO and LUMO – Figure 3c and Figure 3d respectively – show a more spread wave function amplitude throughout the whole surface of the cluster anion: the secondary electron in Al_{39}^{-2} should thus be attached to the monoanion more easily as shown by a larger positive value of EA2 due to the less localized nature of both the additional electron in Al_{39}^{-1} and also the delocalized nature of the 'hole' electron density in the first virtual orbital (LUMO).

We turn now to the estimation of reactivity in the aluminium clusters included in this work. The chemical potential, chemical hardness and softness, and reactivity indices have been used by a number of workers to assess a priori the reactivity of chemical species from their intrinsic electronic properties [35]. Various methods have included atomic charge computation, free valency, spin populations, and the Laplacian of the charge density, among others. Perhaps one of the most successful and best known methods is the frontier orbital theory of Fukui [36, 37]. Developed further by Parr and Yang [38], the method relates the reactivity of a molecule with respect to electrophilic and nucleophilic attack to the charge density. These so-called Fukui functions (FF) are a qualitative way of measuring and displaying the reactivity of regions of a molecule. Specifically, we use the $f^+(\vec{r})$ FF, which measures the sensitivity of the charge density, $\rho(\mathbf{r})$, with respect to the gain of electrons via the expression:

$$f^+(\vec{r}) = \frac{1}{\Delta N}\left(\rho_{N+\Delta}(\vec{r}) - \rho_N(\vec{r})\right) \quad (5)$$

The expression $f^+(\vec{r})$ measures changes in the density when the molecule gains electrons and, hence, corresponds to reactivity with respect to nucleophilic attack or electron attachment. Using the finite difference approximation shown in Equation (5), the charge densities are converged to self-consistency for the anion. The FFs are computed using the finite difference approximation and the self-consistent charge densities for the anion. Figure 4 shows isosurfaces of the positive Fukui function $f^+(\vec{r})$ plotted on aluminium cluster monoanions Al_{23}^- and Al_{39}^- (Figure 4a and Figure 4c) and a mapping of the same function onto an isodensity surface of the electron density in each cluster (Figure 4b and Figure 4d). As depicted in Figure 4, the most likely region where electron attachment should take place corresponds to the vertices of the clusters.

The description of the all-electron DFT optimized geometries of the neutral, monoanionic and dianionic aluminium clusters included in this work are available on request to the authors.
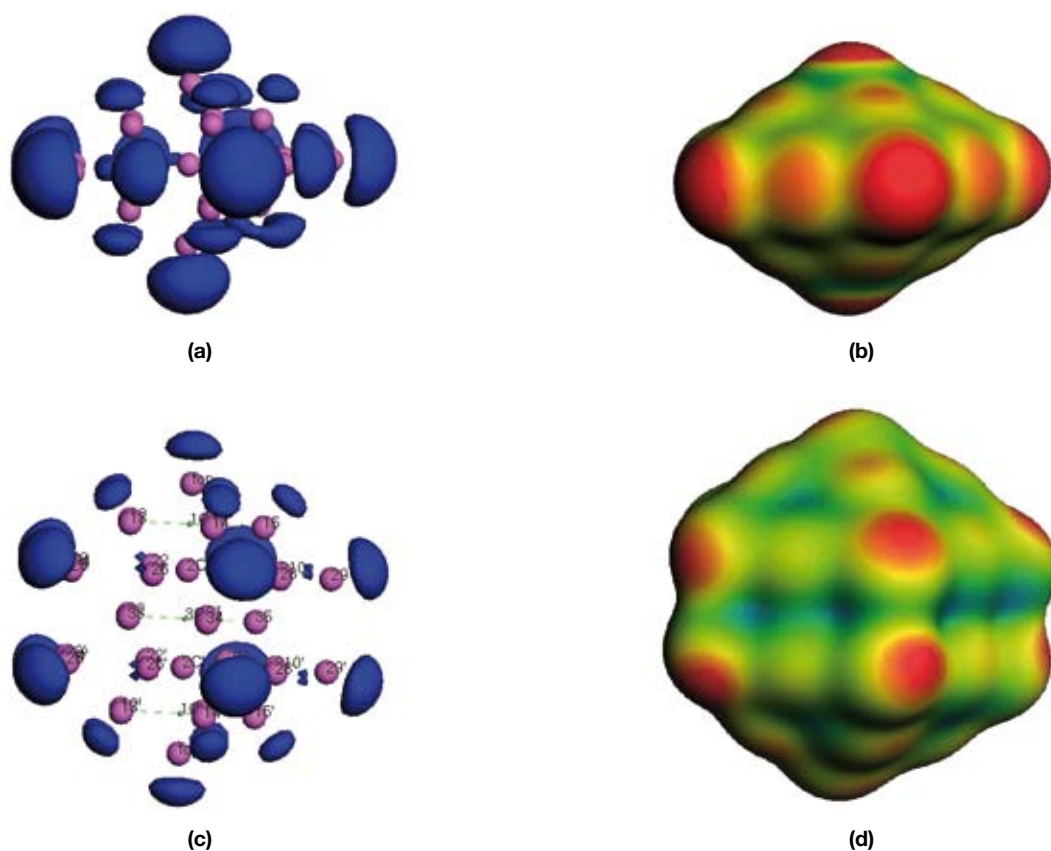

(a)

(b)

(c)

(d)

Figure 4. *Fukui positive functions $f^+(\vec{r})$ for monoanionic aluminium clusters. (a) Fukui positive function $f^+(\vec{r})$ in Al_{23}^-. (b) Fukui positive function $f^+(\vec{r})$ superimposed on an electron density plot for Al_{23}^-. (c) Fukui positive function $f^+(\vec{r})$ in Al_{39}^-. (d) Fukui positive function $f^+(\vec{r})$ superimposed on an electron density plot for Al_{39}^-. Cutoff values for electron density and Fukui function: 0.025 e/Å^3 and 0.0025 e/Å^3 respectively.*

3.2 Comparison of Second Electron Affinities (EA2) Computed with the Charged Conducting-Sphere Model and All-Electron Quantum-Mechanics

3.2.1 Electron affinities (EAs): The second EAs (EA2) of a range of aluminium cluster sizes are plotted in Figure 5. The all-electron DFT calculations were performed for clusters containing 13, 18, 23, 39 and 55 atoms and the classical approximations of the electron affinity by means of the charged conducting-sphere model are computed for clusters containing 10 to 60 atoms using Equation 2.

It is evident from Figure 5 that the electron affinities of a given cluster size as calculated using DFT are more positive than those approximated for the same size using the charged conducting-sphere model. As a result, the expected appearance size for aluminium cluster dianions expected from DFT calculations is smaller than the predictions of the classical model. If the criterion for dianion creation is that the precursor monoanion must have a positive electron affinity, then the quantum mechanical electron affinity computations above suggest that the smallest aluminium cluster dianions should be Al_{23}^{2-} (taking the electron affinities alone into account) (Figure 5: spheres). In contrast to this, the classically predicted dianion appearance size is Al_{33}^{2-} (Figure 5: solid line).

The discrepancy between the electron affinities calculated using the quantum mechanical and classical values is not at all surprising. The classical model is an over-simplification that assumes the cluster to be spherical in shape. Such an assumption is sometimes reasonable in the case of a cluster with a closed electronic shell. However, in most instances such an assumption is invalid. The DFT computations are performed by determination of the lowest energy aluminium structure which is then used to calculate the values of electron affinities, ionisation potentials and other properties of the cluster. The values obtained are therefore for a single structural geometry and are considered to be a reasonable approximation of the true values (i.e. when more than one geometry is considered). For these calculations all clusters were considered to have D_{5h} symmetry with the exception of Al_{13} which was considered to have I_h symmetry [39]. As a final note regarding the shape of a cluster, it is necessary to mention that in the case of open-shell clusters, a sphere is a particularly unsuitable description because those clusters are unstable towards distortions due to the Jahn-Teller effect [40]. In general, a cluster is better described as being ellipsoidal in shape [41].

A further source of disagreement between the results of the rigorous DFT calculations and the classical model is due to the fact that the all-electron quantum mechanical computations account for the interaction of electrons with one another (exchange and correlation effects) whereas the classical model completely neglects this. The only interaction to be considered in the classical treatment is that between the charged-conducting sphere and the approaching point charge (electron). In spite of the aforementioned differences, reasonable agreement between the two models can be achieved by redefining the radius of the cluster to account for an effective electronic charge radius that exists due to spill-out of the electronic wavefunctions beyond

$$R_{cluster} = R_{atom}n^{1/3}. \quad (6)$$

The 'spill-out effect' [33] is a quantum mechanical effect in which the valence electron density is considered to have
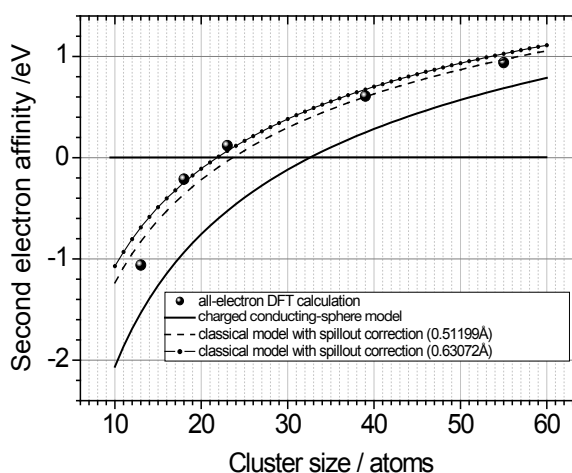

Figure 5: *Second electron affinities of aluminium clusters as a function of cluster size calculated using all-electron DFT calculations (spheres) (Section 3) and the classical charged conducting-sphere model (solid line) (Section 2). Inclusion of a spill-out correction in the classical calculations of the cluster radius yields better agreement between the quantum mechanical and classical models (see text for details).*

a quantum mechanical tail that falls off exponentially in the region outside the radius of the sphere. The effective cluster radius is then considered to be δ larger than that defined above in Equation 6:

$$R_{cluster} = R_{ws}n^{1/3} + \delta \quad (7)$$

where n is the number of atoms in the cluster, R_{ws} is the Wigner-Seitz radius of the atom that composes the cluster and δ is the extent of electron spill-out outside the cluster radius. As the results plotted in Figure 5 demonstrate, the smaller the radius of the cluster, the lower is its electron affinity.

Modification of the classical equation to correct for the electronic spill-out effect is achieved by performing a χ-squared fit of the classical equation to the second electron affinity values obtained via DFT. If a fit is made to all EA2's obtained via DFT, a spill-out factor of 0.51199 Å is obtained. If instead, the doubly magic Al_{13}^- is not used for the fit, a spill-out factor of 0.63072 Å is obtained. Typical values that have been suggested for the spill-out factor (δ) of aluminium range from 0.70 Å – 0.79 Å [33] and 0.54 Å – 1.1 Å [42,47]. Comparing these values with our estimates of a spill-out factor, it is clear that the first estimate of 0.51199 Å is slightly lower than this range of values but the second estimate (obtained by neglecting the electron affinity of the doubly magic Al_{13}^- cluster) of 0.63072 Å is well within this range.

3.2.2 Coulomb barriers

The Coulomb barriers of aluminium monoanions as obtained from the DFT computations have also been compared to those values obtained from the classical model. As mentioned above in the case of electron affinities, the cluster radius is estimated to be larger when the electronic spill-out effect is included. If a value of 0.63072 Å is used for the spill-out factor (dotted line), the heights of the Coulomb barriers of both monoanions in Figure 6 are found to be in better agreement with the DFT values. The Coulomb barrier as computed without the spill-out effect is also included in Figure 6 (solid line) for comparison.
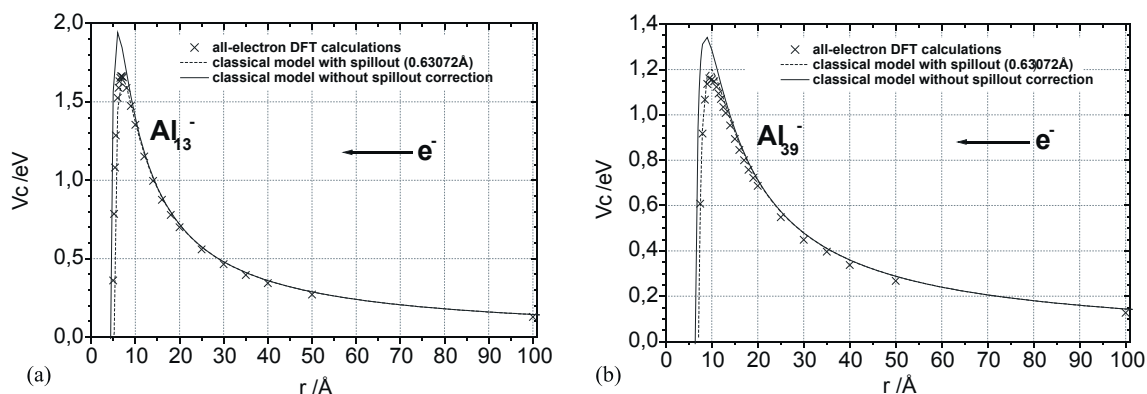
Figure 6. *The Coulomb barriers of (a) Al_{13}^- and (b) Al_{39}^- calculated using all-electron DFT calculations (crosses) are compared with the classical results from the charged conducting-sphere model obtained with (dashed line) and without (solid line) inclusion of an electronic spill-out effect of 0.63072Å. Computations with the hybrid Hartree-Fock – DFT model known as B3LYP, with the 6-31G(d) basis set of double-zeta quality and an additional set of polarization functions for the aluminium atoms.*

Even better agreement is obtained between quantum mechanical and classical results if the spill-out factor is set to the lower value of ~ 0.52 Å in the case of Al_{13}^- and a higher value of ~ 0.75 Å for the larger Al_{39}^- cluster. It has previously been observed that the value of δ is almost independent of cluster size [43, 44] and hence the spill-out factor is expected to have an approximately constant value independent of the radius of the cluster. Hence, we use δ = 0.63072 Å, which was obtained from a χ-squared fit of the classical equation to the DFT values of the second electron affinities of Al_{18}, Al_{23}, Al_{39} and Al_{55} because, not only does it lie between the two extremes (0.52 Å and 0.75 Å), but it also lies within the range of previously suggested values [23, 40, 41, 45].

4. CONCLUSIONS

This work provides a computational work on the expected appearance size, *n,* of dianionic aluminium clusters, Al_n^{2-}. With the sole criterion that an aluminium cluster monoanion must have a positive electron affinity in order to attach a second surplus electron, the all-electron quantum-mechanical DFT computations predict that doubly negative aluminium clusters will be observed for n ~ 23. In contrast to this, the second electron affinity values estimated using the classical charged conducting-sphere model (neglecting electronic spill-out) suggest that a cluster containing n ~ 32 atoms will form a dianionic aluminium cluster. If however, the spill-out of valence electron density beyond the radius of the sphere is taken into account, the effective radius of the cluster is found to be larger than previously considered with the result that the second electron affinities will be more positive than those obtained without consideration of the spill-out effect. An estimate of the extent of this electronic spill-out can be obtained if it is assumed that the disagreement between the two models is due solely to neglect of electronic spill-out in the classical treatment. An estimate of δ = 0.63072 Å, was found to give the best agreement between the computed EA2s with DFT and the charged conducting-sphere classical model. This value lies within the range of previously estimated values of δ.

If the classical charged conducting-sphere model is further developed to account for both the stabilising effect of the Coulomb barrier and the possibility of electron loss

via quantum mechanical tunnelling through the Coulomb barrier of the monoanion, it is found that the estimated dianion appearance size shifts to smaller values. The new charged conducting-sphere classical estimates for the appearance sizes of Al_n^{2-} are then n ~ 29 atoms (for a dianion with a lifetime of 1s) when the spill-out effect is neglected in the estimate of the cluster radius and n ~ 19 when a spill-out factor of δ = 0.63072Å is used to estimate the effective cluster radius. Aluminium cluster dianions ranging in size from Al_{34}^{2-} to Al_{44}^{2-} were experimentally observed at the ClusterTrap experiment recently [14]. The relative dianion yield was found to increase rapidly over a small size range (Al_{37}^{2-} and Al_{40}^{2-}) and a small abundance (~1%) of dianionic clusters were observed for the size range 34 ≤ n ≤ 37 atoms. A number of factors should be considered when comparing experimental observations with theoretical predictions. With regards to the DFT computations, it is important to note that the second electron affinities are computed under an assumption of idealised conditions - The cluster is considered to be isolated such that it undergoes no interaction between itself and other clusters, particles or electromagnetic fields and the computations are also performed at the idealized conditions of T = 0 K (i.e. the computed energies do not contain a temperature correction). The classical estimates too are incapable of providing an exact value of the dianion appearance size. The charged conducting-sphere model uses a number of assumptions and simplifications and thus should only be considered to provide a rough estimate of the expected dianion appearance size. Furthermore, the estimate of the spill-out factor that is used to calculate an effective cluster radius is also obtained following an assumption and thus it is also not considered to be exact.

Finally, a simple calculation of the polyhedral volumes (with aluminium nuclei taken as the vertices) of the clusters Al_n^{-z} with $z = \{0, 1, 2\}$ and $n = \{13, 18, 23, 39, 55\}$ shows a cage expansion on electron addition for Al_{18}, Al_{39} and Al_{55}:

$$V(Al_n^0) < V(Al_n^{-1}) < V(Al_n^{-2}) \quad (8)$$

In contrast to those aforementioned cluster sizes, addition of an electron to neutral Al_{13}, results in a decrease of the cluster volume (ΔV ~ −0.4 Å^3) and electron attachment to neutral Al_{23} does not influence the volume of that particular cluster. For all other cases, in which an electron is attached to neutral and monoanionic clusters, an increase in

the polyhedral volumes by 0.5 Å^3 – 2.0 Å^3 is observed (the increase is observed to a greater extent on addition of the second surplus electron as compared to the monoanion).

5. ACKNOWLEDGMENTS

6. BIBLIOGRAPHY

(Endnotes)
1. H. Haberland (Ed), *Clusters of Atoms and Molecules*, Vols. I and II (Springer, Berlin 1994).
2. R.E. March, *Ion Traps*, in *The Encyclopedia of Mass Spectrometry*, Vol. 1, Ed P.B. Armentrout (Eds.-in-chief M.L. Gross, R. Caprioli, Elsevier, 2003).
3. *Aluminium clusters* by M.F. Jarrold, *in "Clusters of Atoms and Molecules I: Theory, Experiment, and Clusters of Atoms"*, (Springer Series in Chemical Physics 52, Hellmut Haberland (Ed), 1994).
4. *Experiments on Cluster Anions*, K.H. Bowen Jr & E.W. Schlag, from *Encyclopedia of Mass Spectrometry,* Vol. 1, pp 736-751, Ed. P. Armentrout, (Elsevier, 2003).
5. R. Ahlrichs, S.D. Elliott, Phys. Chem. Chem. Phys. **1**, 13 (1999).
6. B.K. Rao and P. Jena, J. Chem. Phys. **111**, 1890 (1999).
7. R. L. Hettich, J. Am. Chem. Soc. **111**, 8582 (1989).
8. X. Li, H. Wu, X.-B. Wang, L.-S. Wang, Phys. Rev. Lett. 81, 1909 (1998).
9. J. Akola, M. Manninen, H. Häkkinen, U. Landman, X. Li, L.-S., Wang, Phys. Rev. B **62**, 13216 (2000).
10. *Atomic Clusters*, in *The Chemical-Physics of Solid Surfaces*, Vol. 12, Ed. D. Woodruff, Elsevier (2007).
11. X. Li, A.E. Kuznetsov, H.-F. Zhang, A.I. Boldirev, L.-S. Wang, Science **291**, 859 (2001).
12. D.E. Bergeron, A.W. Castleman Jr, T. Morisato, S.N. Khanna, Science **304**, 84 (2004).
13. D.E. Bergeron, P.J. Roach, A.W. Castleman Jr., N. O. Jones, S.N. Khanna, Science **307**, 231 (2005).
14. (a) N. Walsh, F. Martinez, G. Marx, and L. Schweikhard, Eur. Phys. J.D 43, 241 (2007). (b) N. Walsh, F. Martinez, G. Marx, L. Schweikhard and F. Ziegler, Eur. Phys. J. D. 52, 27 (2009). (c) N. Walsh, F. Martinez, G. Marx, L. Schweikhard, and F. Ziegler, J. Chem. Phys. 132, 014308 (2010).
15. (a) B. Delley, J. Chem. Phys. **92**, 508 (1990). (b) B. Delley, J. Chem. Phys. **113**, 7756 (2000).
16. Accelrys, *Materials Studio Modeling, Release 4.0*, (Accelrys Software, Inc.: San Diego, 2006).
17. J.P. Perdew, K. Burke, M. Ernzerhof, Phys. Rev. Lett. **77**, 3865 (1996).
18. J.P. Perdew, Y. Wang, Phys. Rev. B. **33**, 8800 (1986).
19. A.D. Becke. J. Chem. Phys. **88**, 2547 (1988).
20. J. Andzelm, King-Smith, G. Fitzgerald. Chem. Phys. Lett. **335**, 321 (2001).
21. E.B. Wilson, J.C. Decius, P.C. Cross, *Molecular Vibrations*, (Dover, New York 1980).
22. P.v.R. Schleyer, Editor-in-Chief, *Encyclopedia of Computational Chemistry*, 5 Volúmenes (Wiley & Sons, 1998).
23. J.D. Jackson, *Classical Electrodynamics*, 3rd Ed., 57-62 (Wiley and sons Inc., USA, 1998).
24. M. Astruc Hoffmann, G. Wrigge, B. v. Issendorff, Phys. Rev. B **66**, 041404 (2002).
25. Ch. Kittel, *Einführung in die Festkörper-Physik, 14th* Ed. (Oldenbourg Verlag, München, Wien, 2006).
26. N.W. Ashcroft, N.D. Mermin, *Solid State Physics.* (Thomson Learning, UK, 2005).
27. A. Herrmann., E. Schumacher, E. Wöste, J. Chem. Phys. **68**, 2327 (1978).
28. L. E. Brus, J. Chem. Phys. **79**, 5566 (1983).
29. D. M. Wood, Phys. Rev. Lett. **46**, 749 (1981).
30. J. M. Smith, Am. Isnt. Aeronaut. Astronaut. J. **3**, 648 (1965).
31. M. Seidl, J. P. Perdew, Phys. Rev. B. **50**, 5744 (1994).
32. G. Makov, A. Nitzan, L. Brus, J. Chem. Phys. **88**, 5076(1988).
33. atomic radius of Al atom as taken from: http://periodic.lanl.gov/default.htm
34. W.A. de Heer, P. Milani, A. Chatelain, Phys. Rev. Lett. **63**, 2834 (1989).
35. W. Yang, R.G. Parr, Proc. Nat. Acad. Sci. USA **82**, 6723 (1985).
36. K. Fukui (1973) *Theory of Orientation and Stereoselection* (Springer, Berlin).
37. K. Fukui, Science **217**, 747 (1982).
38. R.G. Parr, W. Yang, Density Functional Theory of Atoms and Molecules, (Oxford University Press, New York 1989).
39. We should emphasize that we tried to use several point-group symmetries in the geometry optimization of a given cluster, and included in this work only those that gave no imaginary frequencies regardless for the value of $z = \{0, 1, 2\}$ in Al_n^{-z}, within a given point-symmetry group. A comprehensive search of the global energy minimum for a given cluster as function of z is out of the scope of this work.
40. W.A. de Heer, Rev. Mod. Phys. **65**, 611 (1993).
41. K. Clemenger, Phys. Rev. B **32**, 1359 (1985).
42. A. Kiejna, Phys. Rev. B **47**, 7361 (1993).
43. G. Makov, A. Nitzan, L. Brus, J. Chem. Phys. **88**, 5076 (1988).
44. D.R. Snider and R.S. Sorbello, Phys. Rev. B **28**, 5702 (1983).
45. J.P. Perdew, Phys. Rev. B **37**, 6175 (1988).